

The Vortex Shedding Control of Circular Cylinder by Perforated Fairing in Shallow Water

¹Tahir Durhasan, ¹Engin Pınar, ²Muhammed M. Aksoy, ¹Göktürk M. Özkan, *¹Hüseyin Akıllı and ¹Beşir Şahin
*¹Faculty of Engineering and Architecture, Department of Mechanical Engineering Çukurova University, Turkey
²Faculty of Engineering, Department of Energy Systems Engineering Osmaniye Korkut Ata University, Turkey

Abstract

The present experimental investigation was carried out using perforated fairing to control the vortex shedding downstream of the circular cylinder of five different diameter ($D_i=40$ mm, 50 mm, 60 mm, 70 mm and 75 mm) in shallow water using Particle Image Velocimetry (PIV) technique. Arc angle of cylindrical perforated shell ($\alpha=120^\circ$) and porosity of shell ($\beta=0.5$) were kept constant through the experiments. If cylindrical perforated shell becomes a whole circle, its diameter gets value of $D_o=100$ mm and Reynolds number based on the outer diameter ($D_o=100$ mm) as $Re=10000$. Perforated the fairing was positioned concentrically with respect to the circular cylinder (D_i) along its downstream direction. The time-averaged contours of vorticity, $\langle T \rangle$ and Reynolds shear stress, $\langle uv \rangle$ were presented. Streamlines and turbulence statistics were also used to explain the flow structure. It was found that perforated fairing has a significant effect on the flow structure. Suppression of vortex shedding was achieved when compared with the bare cylinder case by perforated fairing. The peak magnitude of Reynolds shear stress, $\langle uv \rangle$ were remarkably decreased and significant extension in the near wake of cylinder were observed for the diameter ratio of $D_i/D_o=0.5$.

Key words: PIV, flow control, vortex shedding

1. Introduction

Suppression of vortex shedding behind a circular cylinder has received much attention due to its potential applications in various fields. Numerous studies on the suppression of vortex shedding have been carried out. Some of these studies have been performed with the active control techniques which bases on using principle of external energy, others have been performed with the passive control techniques which bases on using principle of modifying the geometry. Chen and Aubry [1] developed an efficient active control algorithm for suppression of vortex shedding behind the cylinder in an electrically low-conducting fluid. They used control actuators exert Lorentz forces that localized two different surface of the cylinder. They introduced that the vortex shedding behind the cylinder weakens and eventually disappears completely in both position of the actuators when the Lorentz force is sufficiently large. Ray and Christofides [2] focused on two-dimensional, incompressible viscous channel flow over an infinitely long cylinder and examined effect of controlled rotational cylinder oscillation in reducing the drag exerted on the

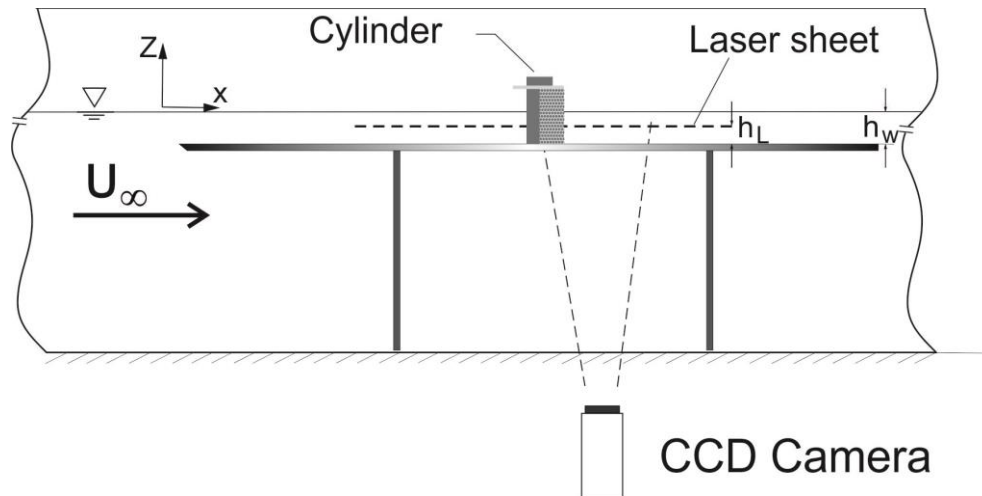
*Corresponding author: Address: Faculty of Engineering and Architecture, Department of Mechanical Engineering Çukurova University, 01330, Adana TURKEY. E-mail address: hakilli@cu.edu.tr, Phone: +903223386945-2730

cylinder. They reported that the drag exerted on the cylinder consistently reduce for Reynolds numbers in the range of $Re=100-500$. Jukes and Choi [3] experimentally studied and they found that the localized plasma around the cylinder can significantly alter the vortex shedding in the wake of the cylinder for Reynolds number of $Re=6500$. Most dramatic effects were observed when the plasma was located very close to the natural laminar separation point. Gozmen et al. [4] demonstrated that the mean flow and turbulent quantities change significantly with sizes of the splitter plates in shallow flow in consequence of the prevention of interaction of shear layers located on both sides of the cylinder. Sudhakar and Vengadesan [5] numerically investigated the vortex shedding characteristics of a circular cylinder an oscillating wake splitter plate. They observed three different patterns of vortex shedding in the wake of the circular cylinder depending upon the frequency and amplitude of plate oscillation: normal shedding, chain of vortices and shedding from splitter plate. Their study also indicated that vortex shedding can be completely suppressed by a short splitter plate ($L/D=1$) if it is given a simple harmonic oscillation at very low oscillating frequencies. If the plate is held stationary, such a suppression requires a plate of length equivalent to five times that of diameter of the cylinder ($L/D=5$). Ikeda and Takaishi [6] showed that the stable wake shear layers of the perforated cylinder and suppression of Aeolian tone are carry out due to the jets emitted from the holes at regular intervals. The flow through screens is also an important issue in order to understand their effect on the flow control since they will be used throughout this study. Oruç [7] studied flow control around circular cylinder with a screen which had a streamlined shape. PIV measurements have indicated that the surrounding of cylinder with a screen significantly suppressed the vortex shedding from the outer cylinder. Ozkan et al. [8] investigated that the change in flow characteristics downstream of circular cylinder surrounded by a permeable cylinder in shallow water using particle image velocimetry technique. They observed that the peak magnitude of turbulent kinetic energy and Reynolds stress decrease remarkably due to the presence of the outer cylinder compare with natural cylinder case. Galvao et. al. [9] used two-dimensional hydrofoils to reduce vortex-induced vibrations (VIV) and drag on the cylinder of circular cross-section. Their parametric search shows that it is possible to completely eliminate vibrations and reduce the drag coefficient to about $C_d=0.5$ at sub-critical Reynolds number. Boorsma et. al. [10] performed experimental study to investigate and optimize the effect of different perforated fairing on the noise control at different location. The fairing self-noise is reduced remarkably by breakdown of the vortex shedding process, resulting in a reduction of associated broadband noise level.

Aim of this study is to investigate the effect of perforated fairings on control of the vortex shedding downstream of the circular cylinder for five different diameter values of cylinder. Results from PIV measurements were compared with each other, as well as with the bare cylinder case.

2. Materials and Method

Experiments were conducted in a closed-loop water channel and a width of 1000 mm, a length of 8000 mm and a free-surface height of 750 mm located at Cukurova University. The flow motion was provided by a centrifugal pump with a speed control unit. Circular cylinders (D_i) of five different diameter values ($D_i=40$ mm, 50 mm, 60 mm, 70 mm and 75 mm) were used in order to investigate the effect of diameter ratio (D_i/D_o) on the unsteady flow structure created in the near wake of the circular cylinder. The porosity ratio, β , is defined as the ratio of the gap area on the whole body surface area. Arc angle of cylindrical perforated shell ($\alpha=120^\circ$) and porosity of cylindrical shell ($\beta=0.5$) were kept constant through the experiments. If perforated cylindrical shell becomes a whole circle, its diameter gets value of $D_o=100$ mm and Reynolds number based on the outer diameter (D_o) as $Re=10000$. Perforated the fairing was positioned concentrically with respect to the circular cylinder (D_i) along its downstream direction. All measurements were done on plan view for water height of $h_w=50$ mm which corresponds to the Froude number of $Fr=0.14$, laser sheet was located parallel to the bottom of the water channel at $h_L=25$ mm for each case. The schematic diagram of water channel and experimental arrangements are given in Fig. 1.



a) Experimental system for side view

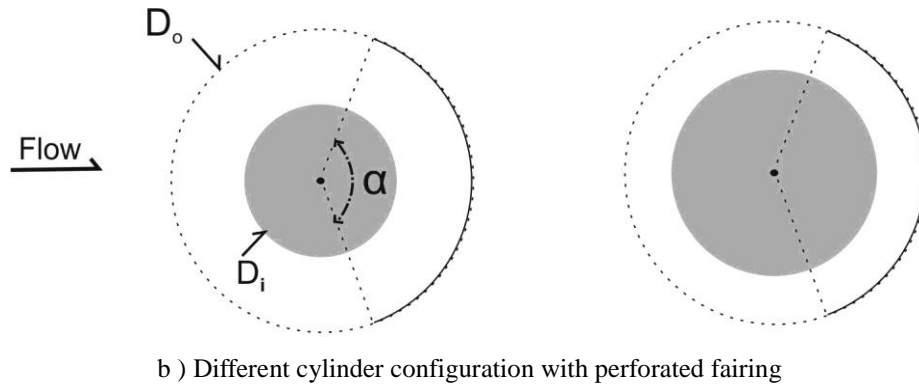


Figure 1. Illustration of basic experimental system and cylinder-perforated fairing configuration

The experiments were performed and the measured data were processed using Dantec Dynamics PIV system and FLOW MANAGER Software installed on a computer. The illumination of measurement field was supplied with a thin and an intense laser light sheet by using a pair of double-pulsed Nd:YAG (yttrium aluminum garnet) laser source energy level of 120 mJ at 532 nm wavelength. The time interval between pulses was 1.75 ms for all experiments and the thickness of the laser sheet was approximately 2 mm. The time interval and the laser sheet thickness were selected such that the maximum amount of particles in the interrogation window was obtained. The image capturing was performed by an 8 bit cross-correlation charge-coupled device (CCD) camera having a resolution of 1016×1016 pixels, equipped with a Nikon AF Micro 60 $f/2.8 D$ lenses. In the image processing, 32×32 integration window pixels were used and an overlap of 50% was employed. A total of 3844 (62×62) velocity vectors were obtained for an instantaneous velocity field at a rate of 15 frames / s. The field of view of measuring planes covers the downstream of the cylinder with the area of 200mm x 200mm for all configurations and the image magnification was 0.0709 mm / pixel. The water was seeded with 12 μm diameter hollow glass sphere particles. The number of particles in an interrogation area was in between 20 and 25. The uncertainty in velocity relative to depth averaged velocity is about 2% in the present experiments. The instantaneous images were captured, recorded, and stored in order to obtain averaged-velocity vectors and other statistical properties of the flow field. Spurious velocity vectors (less than 3%) were removed using the local median-filter technique and replaced by using a bilinear least squares fit technique between surrounding vectors. All experiments were carried out above a platform, having a length of 2300 mm to obtain fully developed shallow flow conditions.

3. Results

The flow structure downstream of bare cylinder and cylinder-perforated fairing configuration are displayed together to compare to the flow characteristics with existence of the perforated fairing. The first column of letter figures presents the bare cylinder results. Time-averaged vorticity, $\langle T \rangle$ contours and streamline topology, $\langle P \rangle$ are illustrated in figure 2 for the cases of bare cylinder and perforated fairing.

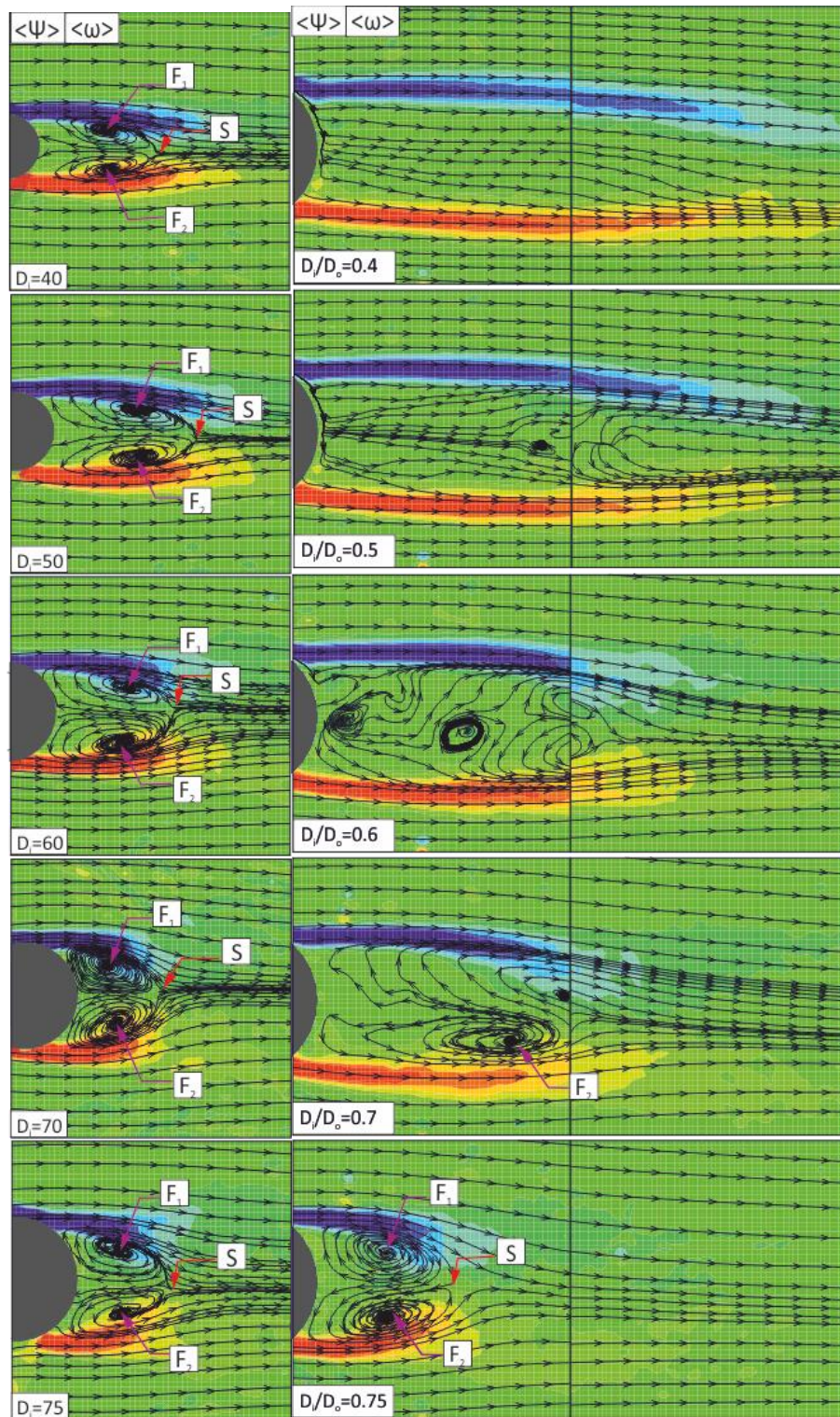


Figure 2. Time averaged vorticity, $\langle T \rangle$ and streamline topology, $\langle P \rangle$ distribution of bare cylinder and cylinder-perforated fairing configuration at different diameter value of the circular cylinder.

Time averaged vorticity contour, $\langle T \rangle$ in the near wake of bare cylinder, which is seen first column of figure 2, is relatively narrow and have a symmetrical structure and also get closer to each other in wake region. It is clearly seen that the shear layers on the both side of cylinder shorten with increasing diameter value of bare cylinder while the magnitude of time averaged vorticity, $\langle T \rangle$ increases. Time averaged streamline topology, $\langle P \rangle$ shows that two well-defined foci points (marked as F1 and F2), which coincide with the centers of streamline swirls, and a saddle point (marked as S), which represents the location of intersection of streamlines are occurred in the near wake of bare cylinder. Presence of perforated fairing significantly effects the flow structure and shear layer extends along downstream direction and gets close to each other in the second field of view up to diameter ratio of $D_i/D_o = 0.75$. Magnitude of time averaged vorticity is also decreased, when compare with bare cylinder case. Two foci points and a saddle point, which occur in the wake of bare cylinder, is completely disappeared at diameter ratio of $D_i/D_o = 0.4$. Although some weak circulation is seen in the wake of diameter ratio of $D_i/D_o = 0.5$ and $D_i/D_o = 0.6$, it is observed that remarkably interaction and stream swirls do not consist as regards bare cylinder cases. This is a distinct evidence of effect of perforated fairing on the suppression of vortex shedding. Perforated fairing starts to become ineffective on the flow structure at diameter ratio of $D_i/D_o = 0.7$ and completely loses its effect at diameter ratio of $D_i/D_o = 0.75$. Two clear foci points and a saddle point occurred in the wake of diameter ratio of $D_i/D_o = 0.75$ similar to the bare cylinder case.

Figure 3 shows Reynolds shear stress, $\langle uv \rangle$ concentrations for the cases of bare cylinder and cylinder perforated fairing configuration. The minimum and incremental values of Reynolds shear stress, $\langle uv \rangle$ contours were taken as ± 0.004 . The solid and dashed lines present positive (counterclockwise) and negative (clockwise) Reynolds shears stresses, $\langle uv \rangle$ respectively. The distribution of positive and negative Reynolds shear stress, $\langle uv \rangle$ is nearly symmetric with respect to the cylinder centerline. While shear layer on the both side of cylinder occurs in the near wake of bare cylinder, shear layers are expanded and the magnitude of Reynolds stress, $\langle uv \rangle$ is decreased with the presence of perforated fairing. The flow emanating through the holes on the fairing causes a jet flow effect, prevents the vorticity on each side of the cylinder by preventing the interaction of vortices thus reducing the momentum entry into the wake region. Therefore, vorticity occurrence and breakage is shifted to the farther regions of downstream flow. As a result, magnitude of Reynolds shear stress, $\langle uv \rangle$ in the wake region reduced when compared with the bare cylinder case. The distance between the circular cylinder and perforated fairing is decreased with the increasing diameter ratio and due to this reason flow entry in to the wake region through the perforated fairing is reduced. Therefore, jet effect of the flow is decreased and vorticity couples interact in a closer region and increase turbulence accordingly. Therefore the magnitude of Reynolds shear stress, $\langle uv \rangle$ tends to increase again and flow structure exhibit like bare cylinder case for $D_i/D_o = 0.75$.

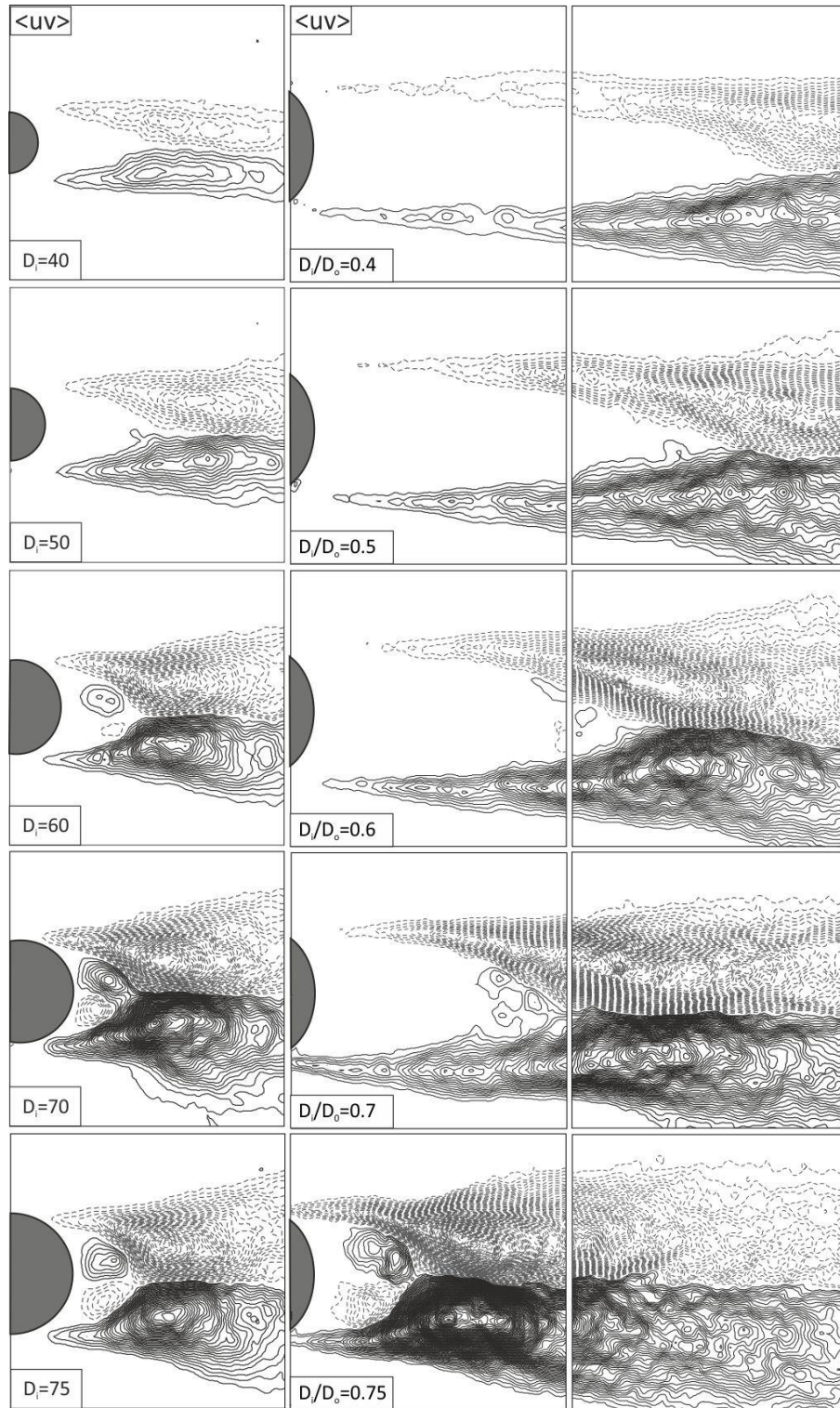


Figure 3. Distribution of Reynolds shear stress, $\langle uv \rangle$ for different bare cylinder and cylinder-perforated fairing combination.

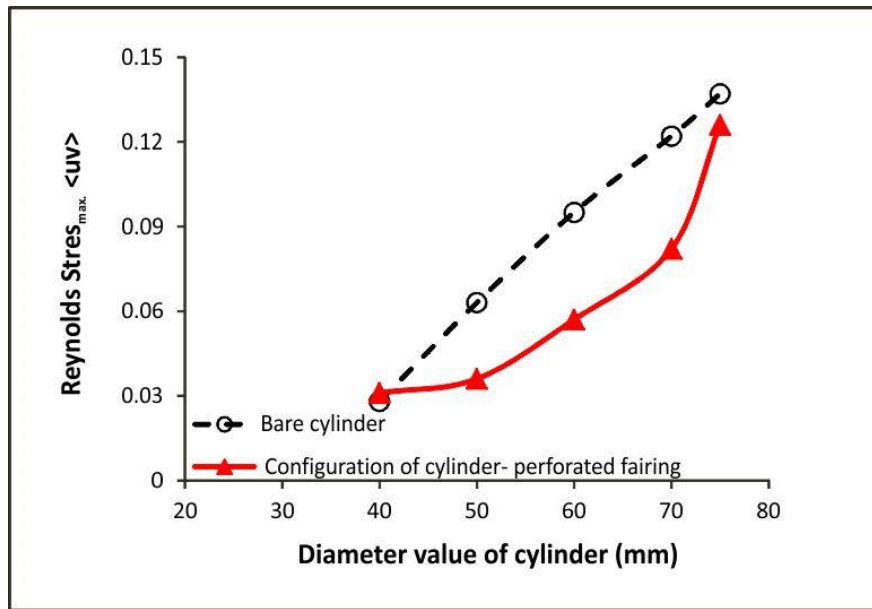


Figure 4. The variation of maximum Reynolds shear stress, $\langle uv \rangle$ with diameter of cylinder

The variation of maximum Reynolds shear stress, $\langle uv \rangle$ with the cylinder diameter are presented in the figure 4 to demonstrate the effect on the turbulence statistics of flow structure. Although the peak magnitude of Reynolds shear stress, $\langle uv \rangle$ of $D_i=40$ is approximately same with the $D_i/D_o=0.4$, it is seen that the point where the peak magnitude of maximum Reynolds shear stress, $\langle uv \rangle$ occurred in further region of cylinder-perforated fairing configuration in the figure 3. Effect of perforated fairing is seen with the increasing diameter ratio and the peak magnitude of Reynolds shear stress, $\langle uv \rangle$ is significantly reduced by %45, %40, %33 for diameter ratios of $D_i/D_o=0.5$, $D_i/D_o=0.6$ and $D_i/D_o=0.7$, respectively. Maximum Reynolds shear stress, $\langle uv \rangle$ of the $D_i/D_o=0.75$ case is close to the bare cylinder case and the decreasing effect on the turbulence statistics at high diameter ratio.

Conclusions

This study was performed to investigate the effect of using perforated fairing on the suppression of vortex shedding in shallow water. In order to explain the flow structure downstream of the circular cylinder, PIV measurements were used and compared by different cylinder cases. The most effective controls were obtained from the case of $D_i/D_o=0.5$. The vortex shedding is controlled by reducing turbulence statistics up to % 45. Furthermore, where it location of the peak magnitude of Reynolds shear stress, $\langle uv \rangle$ was remarkably removed further region of cylinder in this case. The time averaged vorticity contours and streamline topology, $\langle P \rangle$ demonstrate that the suppression of vortex shedding is achieved with using perforated fairing around circular cylinder.

Acknowledgements

I would like to acknowledge the financial support of the Scientific and Technological Research Council of Turkey (TUBITAK) for funding under contract No: 109R001

References

- [1] Chen Z, Aubry N. Active control of cylinder wake. *Communications in Nonlinear Science and Numerical Simulation*; 2005;10;205-216
- [2] Ray P, Christofides D. P. Control of flow over a cylinder using rotational oscillations. *Computer and Chemical Engineering* 2005;29;877-885
- [3] Jukes T, Choi K. S. Active control of a cylinder wake using surface plasma. *IUTAM Symposium on the Unsteady Separated Flows and their Control 2009, IUTAM Book series*; 14.
- [4] Gozmen B, Akilli H, Sahin B. Passive control of circular cylinder wake in shallow flow. *Measurement: Journal of the International Measurement Confederation* 2013, 46(3); 1125-1136.
- [5] Sudhakar Y, Vengadesan S. Vortex shedding characteristics of a circular cylinder with an oscillating wake splitter plate. *Computers & Fluids* 2012;53;40-52
- [6] Ikeda M, Takaishi T. Perforated pantograph horn aeolian tone suppression mechanism. *Quarterly Report of RTRI (Railway Technical Research Institute) (Japan)* 2004; 45(3); 169-174.
- [7] Oruç V. Passive control of flow structures around a circular cylinder by using screen. *Journal of Fluids and Structures* 2012; 33; 229-242.
- [8] Ozkan G. M, Oruc V, Akilli H, Sahin B. Flow around a cylinder surrounded by a permeable cylinder in shallow water. *Experiments in Fluids* 2012; 53(6); 1751-1763.
- [9] Galvao R, Lee E, Farrell D, Hover F, Triantafyllou M, Kitney N, et al. Flow control in flow-structure interaction. *Journal of Fluids Structures* 2008;24;1216-1226
- [10] Boorsma K, Zhang X, Molin N, Chow L. C. Bluff body noise control using perforated fairings. *AIAA Journal* 2009;47